5
Natural Clay Transfiguration using Ni/Co Nanoparticle as Green Catalyst for Efficient Low-Temperature Catalytic Soot Oxidation

Soot particulates in diesel engine exhaust is a severe threat to the environment and human health that causing cancer, affecting heart, lung and mental dysfunctions. Herein, we propose the use of transition metal modified natural clay as an effective green catalyst for its prospective application in the oxidation of soot particles. The Ni and Co (NCS) incorporated natural clay catalysts were prepared by a simple wet impregnation method. The synthesized catalyst samples were meticulously characterized by powder X-ray diffraction (XRD), BET N_2 adsorption-desorption, Transmission Electron Microscope (TEM), Oxygen temperature program desorption (O_2-TPD), Hydrogen Temperature Programmed Reduction (H_2 TPR) and X-ray Photoelectron Spectroscopy (XPS). NCS catalyst showed higher H_2 absorption at a lower temperature with similar trends as observed in O_2 TPD, which indicated good redox property of the prepared catalyst. The catalytic activity, when tested in a TGA (thermogravimetric analysis) furnace, showed low T_{50} at 358 °C, showing excellent catalytic performance. This superior catalytic activity is due to the improved surface oxygen vacancies and thermal stability by the metal modification in clay.

5.1 Experimental techniques

Natural clay was obtained from Barmer in Rajasthan, India which is mostly comprised of montmorillonite.(Tyagi, Chudasama et al. 2006) Nickel nitrate hexahydrate and Co nitrate hexahydrate precursors were purchased from Alfa Aesar.

5.1.1 Methods

Natural clay was processed thoroughly for three times using DI water to remove any impurities present via the method of sedimentation wherein the obtained clay was stirred vigorously and then kept undisturbed to settle down. Afterwards, it was dried in an oven at 120 °C. A 4 % salt of Ni precursor was dissolved in 4N HNO_3 and stirred until it becomes a paste. Finally, after the paste has dried, the catalyst prepared is grinded and calcined at 500 °C under N_2 atmosphere. To make a bi-metal alloy doped clay catalyst similar procedure was adopted for doping with Co. Lastly, the Ni and Co doped clay was calcined under H_2 atmosphere.

5.2 Results and discussion

5.2.1. Clay soot oxidation

The XRD pattern of the nanoparticles as shown in Figure 1a reveal the presence of both montmorillonite and quartz with the highest intense peak at 26.5° for quartz which indicates the laminar stack of the doped clay is intact with proper orientation after subsequent doping with metal nanoparticles similar to undoped clay (Figure 5.1a). The metal presence was not observed as reflections on the XRD pattern corresponding to Ni and Co, which can be due to overlaying with the clay patterns and also minimal weight percentage of Ni and Co precursors compared to clay material. Figure 5.1b represents the XPS survey scan of the NCS and clay. The highlight shows the presence of Ni and Co peaks in NCS catalyst in comparison to clay and thus can confirm the presence of both the metal in the catalyst system. BET measurement was undertaken to analyze the surface property, such as pore width and surface area of the catalyst.

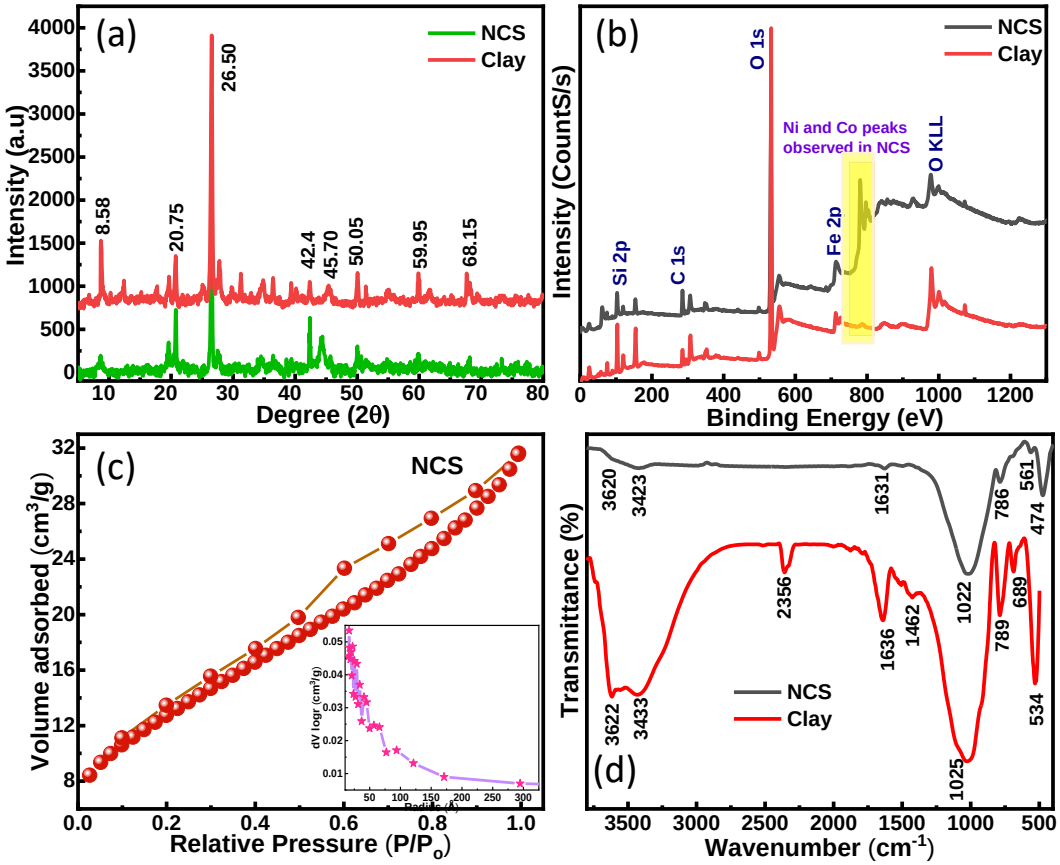

Figure 5.1: XRD pattern of NCS and pristine clay without doping (a), XPS survey scan (b), pore size distribution (inset), and adsorption-desorption isotherm (c) and FTIR spectra (d) of the synthesized catalysts.

The type of behaviour shown by the NCS sample, as shown in Figure 5.1c, is for type II isotherm, which is a characteristic feature of macroporous and non-porous material, which is a type of monolayer formation followed by multilayer adsorption on the surface of the sample. The formation of the multilayer occurs unrestricted in this type of isotherm. As can be seen, at about 0.5 relative pressure, there is an inflection point, which is an indication of the start of multilayer formation and can be called as the knee point. This is a representative of nanoparticles forming plate-like aggregates and unfilled macropores. The plate-like aggregation often leads to the formation of slit-shaped pores. The surface area of the NCS was found to be 46 m^2/g, and the pore size distribution shows pore size around 50 Å (refer Table 5.1). The IR spectrum of the as-synthesized clay and doped NCS is given in Figure 5.1d. The broad peaks at around 3620 cm^{-1} and 3423 cm^{-1} characterizes the presence of structural -OH group and -OH stretching of the water molecule adsorbed on the NCS. The peak at around 1631 can be attributed to the bending of -OH group of the adsorbed water molecules. Broadly, the presence of quartz is identified as the presence of bands in the wavenumber region from 1200 – 500 cm^{-1}. The peaks at around 786 cm^{-1} (and the extra peak at 689 for the as-synthesized clay) and 1022 cm^{-1} can be attributed to the deformation of the Si-O-Si bond. The peak at 561 cm^{-1} and 534 cm^{-1} can be ascribed to Si-O-Al bond in the materials.

Table 5.1. Properties of Catalyst from BET and O_2 TPD.

Sl. No.	Catalyst	Average Pore Size (nm)	BET Surface Area (m^2/g)	O 1s peak deconvolution		H_2 TPR temperature (℃)	H_2 consumption (μmol/g)	Tm Soot Oxidation temperature (℃)
				O_α peak	O_β peak			
1.	Clay	150	44	532.2	-	553 795	219 120	566
2.	NCS	21	46	531.7	529.7	262 470	1103 1688	358
3.	Ni Clay	51		532.3	-	532 607	171 1451	566
4.	Co Clay	26		532.4	530.4	354 425	169 1389	538

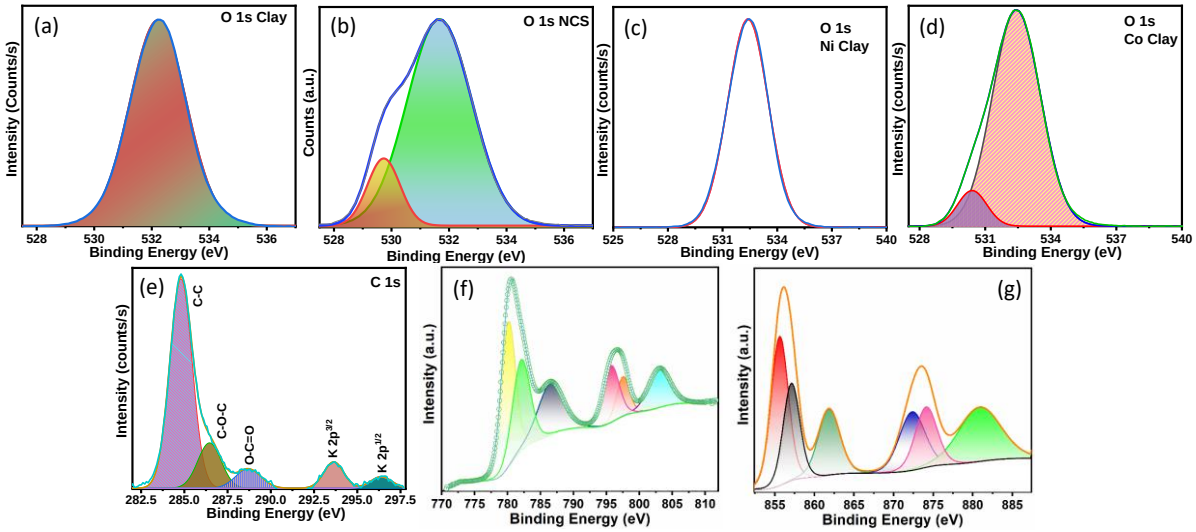

Figure 5.2: High resolution XPS (a, b, c and d) O 1s spectra of clay, NCS, Ni Clay and Co Clay catalyst, (e) C 1s, (f) Co 2p and (g) Ni 2p high resolution scan of NCS catalyst.

The C 1s of NCS catalyst (Figure 5.2e) shows a broad peak that is deconvoluted to five smaller peaks with three peaks at 284.8 eV, 286.4 eV, and 288.69 eV corresponding to C-C, C-O-C, and O-C=O respectively. The peaks at 293.6 eV and 296.38 eV can be related to weaker peaks of K $2p_{3/2}$ and K $2p_{1/2,}$ which occurs overlapping with the C 1s. The O 1s of (Figure 5.2b) high-resolution XPS spectra of NCS are deconvoluted into two peaks at 529.7 eV and 531.6 eV. The former can be assigned to the presence of O^{2-} ions, whereas the latter is a characteristic of weakly adsorbed species and coordination of oxygen species in the subsurface, which indicates the presence of defective metal oxides Ni and Co oxides.(Dupin, Gonbeau et al. 2000) The oxygen species at lower binding energy can be assigned to the lattice oxygen (O_{latt}), and the oxygen species at higher binding energy can be a representative of surface adsorbed oxygen (O_{surf}). It can be observed that the oxygen at lower binding energy is not present in the clay catalyst (Figure 5.2a) compared to the NCS catalyst that showed the presence of lattice oxygen present at a lower binding energy of 529.5 eV. The high-resolution XPS spectra of Co 2p (Figure 5.2f) shows $2p_{1/2}$ and $2p_{3/2}$ spin-orbit splitting. The high intensity Co $2p_{3/2}$ peak at 780.08 eV is deconvoluted and gives two fitted peaks using a Gaussian-Lorentzian function at 780.58 eV and 782.58 eV. The two satellite peak at 787.08 eV and 803.58 eV can be assigned to multiple electron excitation from Co^{2+} and Co^{3+}.(Chen, Kronawitter et al. 2015) This might be an inference of the presence of both divalent oxides and hydroxides in the catalyst.(Liang, Ren et al. 2017) The Ni 2p (Figure 5.2g) can be deconvoluted into two spin-orbit doublets at 856.1 eV and 873.5 eV with peaks at 861.8 eV and 881.46 eV can be assigned to satellite peaks of Ni $2p^{3/2}$ and Ni $2p^{1/2}$ which

is typical of Ni^{2+} peak.(Dutta, Indra et al. 2017)(Zhou, Weng et al. 2017) This indicates the presence of active Ni and Co species (with 0.79 at % and 10.38 at % as detected in the XPS)in the NCS catalyst that helps in soot oxidation.

In addition to the XPS spectra, the O_2 TPD profiles of NCS and pristine clay catalyst (Figure 5.3a and 5.3b) gives an account of the interaction of the catalyst with various oxygen species. Oxygen species can be assigned to four different entities - O_α ($O_{2(ads)}$), O_β ($O_{2^-(ads)}$), O_γ ($O^-_{(ads)}$) and O_δ ($O_2^{2-}{}_{(ads)}$) according to the temperatures at which they get desorbed. The initial desorption for the NCS catalyst might indicate the presence of physisorbed oxygen species on the surface at 240 °C, as shown in Figure 5.3b, which is absent in the clay catalyst Figure 5.3a. This indicates that incorporation of Ni and Co onto the NCS catalyst has led to desorption of O_α. Similar trends can be observed in the chemical analysis using XPS, where the lattice oxygen is absent in the clay catalyst. Both the catalyst showed the presence of O_β ($O_{2^-(ads)}$) and O_γ ($O^-_{(ads)}$) from a temperature range between 400 °C to 600 °C which can be attributed to subsurface movement of O^-. The desorption of O_β and O_γ shows the reducibility of the metal atoms present, which generates oxygen vacancies in the catalyst. The oxygen species desorbing at a higher temperature beyond 600 °C corresponds to the oxygen incorporated on the crystal structure. It can be very observed that the incorporation of Ni and Co onto the NCS catalyst has significantly altered the oxygen desorption in the solid. This can be because instituting new materials will lead to the formation of boundaries and interfaces. Such events will greatly enhance the diffusion of subsurface and bulk oxygen species towards the surface, altering the valency of the lattice constituents, thereby changing the redox property of the catalyst.(Muñoz, Moreno et al. 2014) Moreover, the hydrogen annealing is bound to have created additional defect sites and oxygen vacant species, which is in agreement with XPS and O2-TPD results showing more labile and surface-active oxygen species.

The observed desorption of NCS catalyst showed stronger desorption capacity compared to clay which confirms the improved mobility of lattice oxygen in the former.(Lin, Li et al. 2018) Figure 5.4a illustrates a TEM image of the prepared NCS, showing the morphology, size, and crystallinity of the prepared catalyst. The images in Figure 5.4b and 5.4c show the intercalated clay layer with spacing about an average of approximately 6 nm as marked in the image the shaded and marked portion in Figure 5.4d is the HRTEM, which was analyzed using Gatan digital micrograph to calculate the d spacing value. The IFFT and FFT of planes in a different direction in this region is indicated in Figure 5.4e, 5.4f with corresponding Figure 5.4g and 5.4h, respectively. The d-spacing of 0.45 nm and 0.44 nm, as indicated in Figure 5.4f and 5.4g, corresponds to peak at 19.5 2θ degrees as indicated in XRD Figure 5.1a.

The H_2 TPR studies the reducibility of the catalyst, and it shows two main zones of reduction – one at a lower temperature (below 600 °C) and the other at a higher temperature (above 600 °C). Figure 5.3c is the first-order derivative of the thermograms, which enables the study of the reducibility of the catalyst. The one-step reduction can be accounted as the main reduction peak at around 300 °C for NCS, whereas for clay two-step reduction with the initial step reduction at around 560 °C and the second step at 610 °C can be seen. The peak at 228 °C can be ascribed to overlapping easily reducible Co oxide and Ni oxide via $NiO \rightarrow Ni^{X+}$ and $Co_3O_4 \rightarrow Co^{Y+}$ and the reduction of adsorbed oxygen. Whereas, the highest peak at 264 °C can be accounted for the reduction of $Ni^{X+} \rightarrow$ Ni metal and $Co^{Y+} \rightarrow$Co metal.(Ay and Üner 2015, Palma, Ruocco et al. 2017)

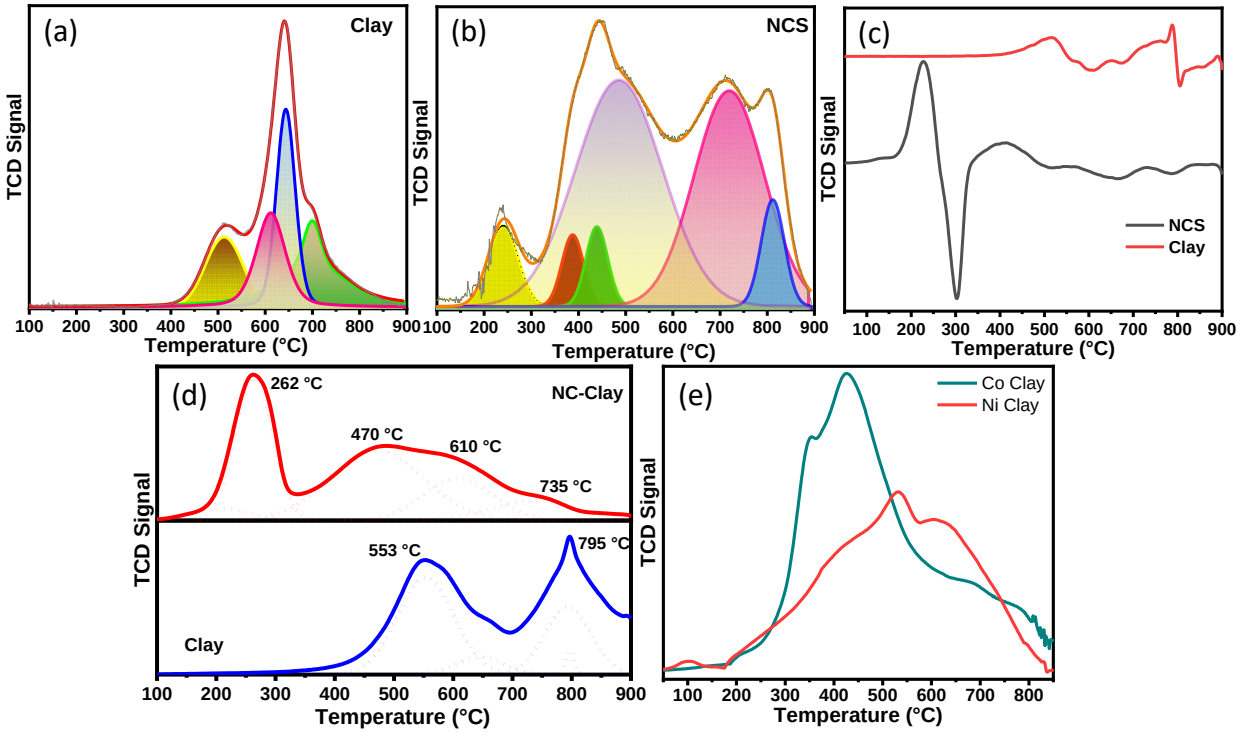

Figure 5.3: High-resolution O_2 TPD of (a) clay and (b) NCS catalyst with its corresponding deconvoluted profile, and 1st order derivative (c) and deconvoluted H_2 TPR (d) thermograms of clay and NCS catalyst and (e) H_2 TPR of Ni clay and Co clay catalyst.

From Figure 5.3e it can be observed that both Ni Clay and Co Clay separately gives reducibility at higher temperature starting from 354 °C for Ni clay to the highest intense peak at 425 °C to a broader peak at a higher temperature. Comparatively, Ni clay showed initial reducibility with a broad peak at around 375 °C, followed by a weakened peak at 532 °C and a broader peak around 607 °C. It is evident that with the introduction of Ni and Co metal on to the clay, there is an increase in reducibility as the oxides of these metal is easily reducible under H2. The use of both the species significantly promotes higher reducibility in the NC-Clay catalyst as compared to when used separately. Hence, it can be inferred that the bimetal (Ni and Co) incorporation in clay makes a better catalyst (as can be seen from the soot oxidation data). The low temperature might be due to the presence of easily reducible oxides of Ni and CoThe details are given in Table 5.1. It is evident that with the advent of the introduction of Ni and Co metal on to the clay, there is an increase in reducibility as the oxides of these metal are easily reducible under H_2. The use of both the species significantly promotes higher reducibility in the NCS catalyst as compared to when used separately, and hence it can be added that the use of Ni and Co in clay makes a better catalyst (as can be seen from the soot oxidation data). The low temperature might be due to the presence of easily reducible oxides of Ni and Co.(Muñoz, Moreno et al. 2014) Figure 5.3d gives the deconvolution of the main species to give relative information of the different species present that can be reduced. The main uptake corresponds occurring at a lower temperature for NCS might be an indication of surface reduction of Co oxide to cobalt. It can also be observed that NCS catalyst when compared to the pristine clay catalyst gets drastically reduced at a lower temperature from 553 °C and 262 °C, which is an indication of the NCS catalytic system promoting good redox property. Moreover, it also signals that the surface has the presence of oxygen species, which are highly mobile with rapid active site regeneration for H_2 adsorption.(Lin, Li et al. 2018) Additionally, there is an observed increase in the intensity of the peak which amounts to increase H_2 consumption. NCS catalyst after deconvolution exhibited the largest peak area at 262 °C with maximum oxygen storage capacity (OSC), which is an important parameter in the catalytic application for storing and releasing of active oxygen species.

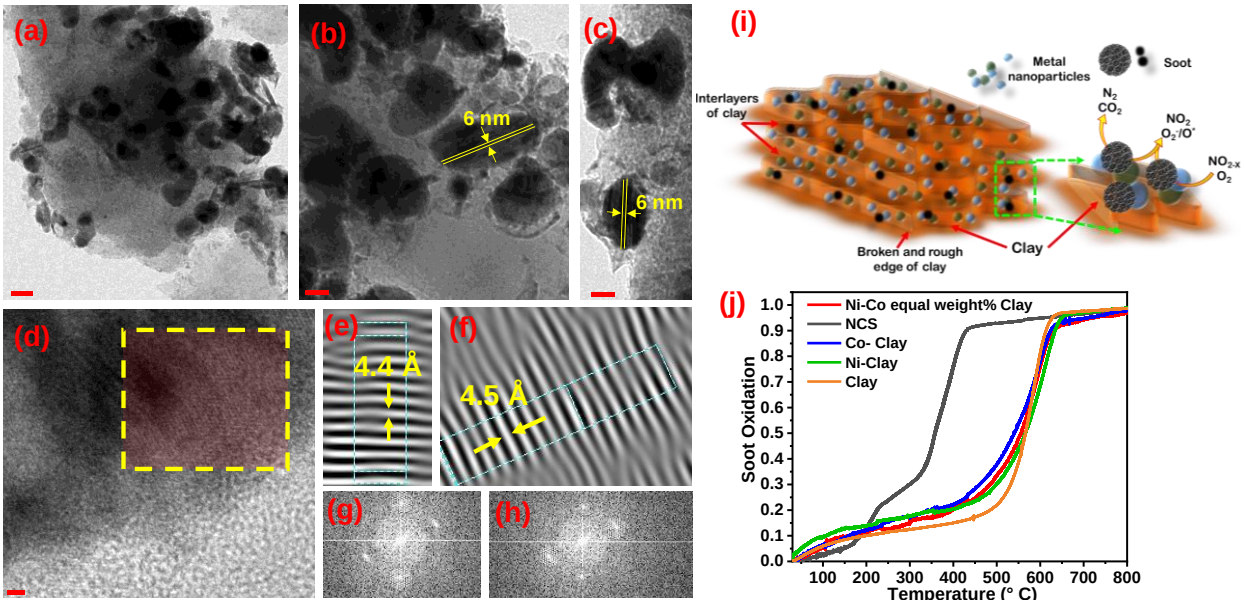

Figure 5.4: TEM image (a, b and c) at different scale, HRTEM image (d) and IFFT image (e and f) with corresponding FFT image (f, h) of the selected area in (e), schematic representation of soot oxidation of NCS catalyst using soot (i) and soot oxidation activity of NCS (j).

TGA is a general method for characterizing the soot oxidation activity of catalyst whereby the catalyst is subjected along with model soot, generally carbon black, a schematic is shown in Figure 5.4j. The average temperature reported in the literature ranges from 400-500 °C for a good soot oxidation catalyst. We are reporting a Ni-Co co-doped over clay catalyst as a novel material for soot oxidation with the T_{50} temperature reduced to 358 °C as shown in Figure 5.4k. The good catalytic activity achieved in this study can be attributed to an increase in surface adsorbed oxygen and improved redox property in the NCS catalyst which agrees well with the chemical analysis data above.

5.3 Conclusion

Natural clay was modified using Ni and Co to catalyst with the clay as support. The introduction of bimetals brought in noticeable changes in the physical, chemical and catalytic properties of the catalyst, which can be considered as a result of the synergistic effect of both metals. The H_2-TPR results suggest good redox property. Moreover, active sites and surface oxygen with labile species help achieve oxidation of soot at T_{50} temperature as low as 358 °C. This is the first study where bi-metal incorporation of Co and Ni has been done in clay for soot oxidation. The correct study creates new possibilities to design catalytic converters of low cost and sustainable with high efficiency.

...